OPEN ACCESS Freely available online

Journal of Geography & Natural Disasters

Research Article

Refinement of Precipitation Distribution in Southern Brazil under the Conditions of the Pacific Ocean Temperature Anomaly

Osvaldo Luiz Leal de Moraes[1*], Jose Marengo Orsini[2]

[1]Department of Climate and Sustainability, Brazilian Ministry of Science and Technology, Brasília, Brazil; [2]National Early Warning and Monitoring Centre for Natural Disasters, São José dos Campos, São Paulo, Brazil

ABSTRACT

The role of the Pacific Decadal Oscillation (PDO) and the El Niño-Southern Oscillation (ENSO) was investigated in relation to anomalous precipitation in Southern Brazil. A daily precipitation dataset was used, covering the period 1961 to 2016 from 106 monitoring stations. In addition, a direct comparison was made between El Niño plus positive PDO events and La Niña plus negative PDO events to discover any correlations between these phenomena in regional precipitation. Our results indicate that significant monthly favorable anomalous precipitation across the region occurred only during intense or extreme El Niño events, and PDO had no modulating effect regardless of its intensity. However, monthly negative precipitation anomalies at higher latitudes ranged from low to moderate during robust La Niña periods, suggesting some association with adverse PDO events.

Keywords: El Niño-Southern oscillation; Pacific decadal oscillation; Precipitation in Southern Brazil

INTRODUCTION

Rainfall has great social and economic importance in Southern Brazil, which has more than 25 million inhabitants and is responsible for 40%, 40%, and 80% of national production of soybeans, corn, and rice, respectively [1]. Mid-latitude systems greatly influence this region, and its geographic location is characterized by well-distributed rainfall throughout the year [2]. However, precipitation variability is considerable, and the effects of large-scale circulation anomalies are evident. The climate of southern Brazil is strongly associated with El Niño–Southern Oscillation (ENSO) phases and the effects of these events on precipitation in the region have been studied in recent decades [3-10]. These studies, confirmed by model experiments, showed that warm episodes of ENSO (El Niño) in Southern Brazil produce precipitation above the climatological mean, while cold episodes (La Niña) produce values below the mean [11-17]. Cai et al. [16] showed that the effects of ENSO are very different due to ENSO diversity and the types of variability within and outside the Pacific Ocean with different ENSO types and the effects of SST variability in the South Atlantic.

The effects of ENSO are complicated by other forms of natural climate variability. These interact and modify the effects and trends of ENSO, such as the Southern Annular Mode (SAM), the Indian Ocean Dipole (IOD), the Pacific Decadal Oscillation (PDO), the Atlantic multidecadal variability, and warming due to the greenhouse effect [18-25]. Overall, Southeastern South America, including Southern Brazil and the northern sector of the northern and Northeastern regions of Brazil, is most affected by teleconnection patterns [26].

ENSO and PDO have a significant impact on global climate and precipitation patterns. Schoennagel et al. [27] analyzed the relationship between ENSO and PDO and fire occurrence due to drought in subalpine forests in the Rocky Mountains. McCabe et al. used first leaf data at 856 sites across North America from 1900–2008 to examine how ENSO and PDO individually and together can influence the timing of spring [28]. Limestone and Goodrich examined the effects of ENSO and PDO on winter air pollution in Phoenix, while Henson et al. conducted an analysis of crop yields in Missouri to determine if there is interannual or multidecadal variation due to ENSO and PDO [29]. Mariano et al. showed strong correlations between ENSO and PDO influences and the likelihood of occurrence of extreme physical conditions that altered fish communities in a shallow lake due

Correspondence to: Osvaldo Luiz Leal de Moraes, Department of Climate and Sustainability, Brazilian Ministry of Science and Technology, Brasília, Brazil, E-mail: osvaldo.moraes@mcti.gov.br

Received: 20-Oct-2023, Manuscript No. JGND-23-27730; **Editor assigned:** 23-Oct-2023, PreQC No. JGND-23-27730 (PQ); **Reviewed:** 07-Nov-2023, QC No. JGND-23-27730; **Revised:** 14-Nov-2023, Manuscript No. JGND-23-27730 (R); **Published:** 21-Nov-2023, DOI: 10.35841/2167-0587.23.13.290

Citation: Moraes OLL, Orsini JM (2023) Refinement of Precipitation Distribution in Southern Brazil under the Conditions of the Pacific Ocean Temperature Anomaly. J Geogr Nat Disasters. 13: 290.

to local climate variability [30]. More recently, Nguyen et al. [31] examined the combined effects of ENSO and PDO on global droughts in terms of magnitude, timing and duration of Gamelin et al. [32] examined the role of ENSO on upper tropospheric and lower stratospheric ozone variability, with a focus on South America, by examining patterns of teleconnections during warm and cool PDO phases. Specific studies discuss the modulating effect of PDO on ENSO precipitation in other regions of the world [33-37]. ENSO is the main coupled mode acting on interannual time scales and modulating tropospheric circulation worldwide. ENSO teleconnections may depend on the phases of PDO and the characteristics of warming over the central and Eastern Tropical Pacific [32]. If ENSO and PDO are in the same phase, El Niño/La Niña may be enhanced. On the other hand, if ENSO and PDO are out of phase, it is suggested that they may offset each other and prevent the effects of ENSO rainfall [16].

More recently, other studies have shown that different phases and "types" of ENSO have significant impacts on monthly and seasonal average precipitation, as well as on the frequency and magnitude of extreme precipitation events in southern South America [38,39], which includes Southern Brazil. During the canonical El Niño (La Niña), there tends to be an increase (decrease) in precipitation in the La Plata basin, while during the El Niño Modoki these typical patterns are not observed and in some regions the anomalies show opposite results [40]. Jimenez et al. analyzed wet and dry episodes associated with El Niño events in tropical South America and found distinct spatial pattern anomalies in precipitation depending on El Niño type (Central Pacific CP *vs*. Eastern Pacific EP) [41].

Other studies focusing on the decadal scale of precipitation variability have pointed to a link between South American climate and PDO [42,43]. Silva et al. looking at the effects of ENSO and PDO in the region, showed that precipitation anomalies increased over southeastern South America when PDO (+) and El Niño were in phase [44]. They indicated that this was a consequence of the intensification of the convergence of moisture fluxes in this region. The ENSO and PDO effects in southern Brazil are usually associated with a significant positive anomaly in monthly precipitation and mean average temperature. In this study, the effects of ENSO and PDO on monthly precipitation were examined using precipitation data from a network of 106 precipitation stations in southern Brazil. No other comparable study has used a meteorological data set like that used in this study. The size of the time series over more than 60 years, with more than 100 monitoring stations with daily precipitation data, makes the results more reliable than those obtained by modelling or interpolating a small number of stations. We used these data to answer several important questions: How do the combined effects of ENSO and PDO affect precipitation in the region?

Do they cause equal impacts? Are their spatial effects homogeneous? We investigated the impact of ENSO and PDO phase combinations on monthly average precipitation in southern Brazil using long-term observational data. A direct comparison was made between El Niño plus favourable PDO events and La Niña plus unfavourable PDO events to discover any modulating effects of PDO on El Niño-related precipitation in this region.

MATERIALS AND METHODS

The database for this study consists of daily precipitation records from 106 stations from 1961 to 2016. The daily observations were used to calculate monthly precipitation values for those years. The dataset is freely available at www.snirh.gov.br on the National Water Agency website (ANA). There are many more rain gauges in southern Brazil, but most of the time series are short or have gaps. The dataset ANA contains climate records from meteorological stations from numerous sources, including the National Institute of Meteorology (INMET). We also used all conventional meteorological stations from INMET (45) and gauging stations from ANA and other sites (61). The criterion for selecting INMET gauging stations was that they were part of the official climatological network of Brazil. Other monitoring stations were selected because they had a sufficiently long time series to cover the same period. All stations that met this criterion were selected for this study. The ANA performed quality control checks before publishing the data on its website. However, INMET's daily precipitation data had a significant number of missing records that have yet to be determined. Therefore, data from other stations in the same community were used to fill in these gaps. For example, the INMET tide gauge (code A865: 27.81306° S, 50.32459° W) in Lages, Santa Catarina State, has gaps from January 1984 to December 1984 and from January 1986 to December 1987. In this municipality, a gauge ANA (code 2850004: 28.1522° S, 50.4408° W) has information for these periods that can be used to fill the gaps in the INMET station data. Because gap filling was sensitive to missing data prior to importing the datasets from this station, the correlation between the data from the two stations was calculated to check for consistency considering all data in the time series, excluding the gaps in both series. For correlations greater than 0.9, the gap was closed by simply inserting the data from the second station. Correlations between 0.75 and 0.89 were corrected mainly to remove bias or spikes, while for correlations below 0.75, no gap filling was done and that time station was omitted. For stations INMET A865 and ANA 2850004, the correlation was 0.905 and was obtained from 418 monthly precipitation measurements. Monthly precipitation is also sensitive to missing data. Therefore, the monthly indices were not calculated for months in which more than three days were missing. The coverage of the area with 106 stations was relatively homogeneous, as shown in Figure 1. Therefore, these stations were suitable for this study.

Two climatic teleconnection indices were considered in this study. The Oceanic Niño Index (ONI) is the standard used by the National Oceanic and Atmospheric Administration (NOAA) to identify El Niño (warm) and La Niña (cold) events in the tropical Pacific Ocean. It shows the rolling three-month mean SST anomaly for the Niño 3.4 region (i.e., 5° N–5° S, 120° W–170° W) and is available at https://origin.cpc.ncep.noaa.gov. NOAA considers El Niño conditions to exist when the Oceanic Niño Index is ≥ +0.5, meaning that the East-Central tropical Pacific is significantly warmer than usual. Conversely, La Niña conditions exist when the Oceanic Niño Index is ≤ -0.5, implying cooler than average conditions. The National Center of Environmental Information (NCEI) PDO index is based on the NOAA Extended Reconstruction of Sea Surface Temperature (ERSST). The ERSST anomalies were regressed on the Mantua PDO index for the overlap period to calculate a PDO regression map for ERSST anomalies in the North Pacific [45]. These anomalies were then projected onto the map to calculate the NCEI index (https://www.ncdc.noaa.gov/teleconnections/pdo/). Contrasting anomalies in SST characterize the PDO: Warmer and colder SSTs than the climatology between the tropical/northeastern and central/northwestern North Pacific on an interdecadal scale. Finally, it

should be emphasised that the word "mean" in this study refers to the value calculated for a particular station. In contrast, the word "mean" is used when the calculated value refers to the totality of stations (i.e., MAP means the monthly average precipitation of all 106 gauges, while MMP is the monthly average precipitation for a particular rain gauge). Figure 2 shows the MAP (black dots) for January 1961 to December 2016 on the vertical axis and the ONI and PDO indices on the horizontal axis. The red dots represent the projection of the black dots onto the ONI-PDO surface.

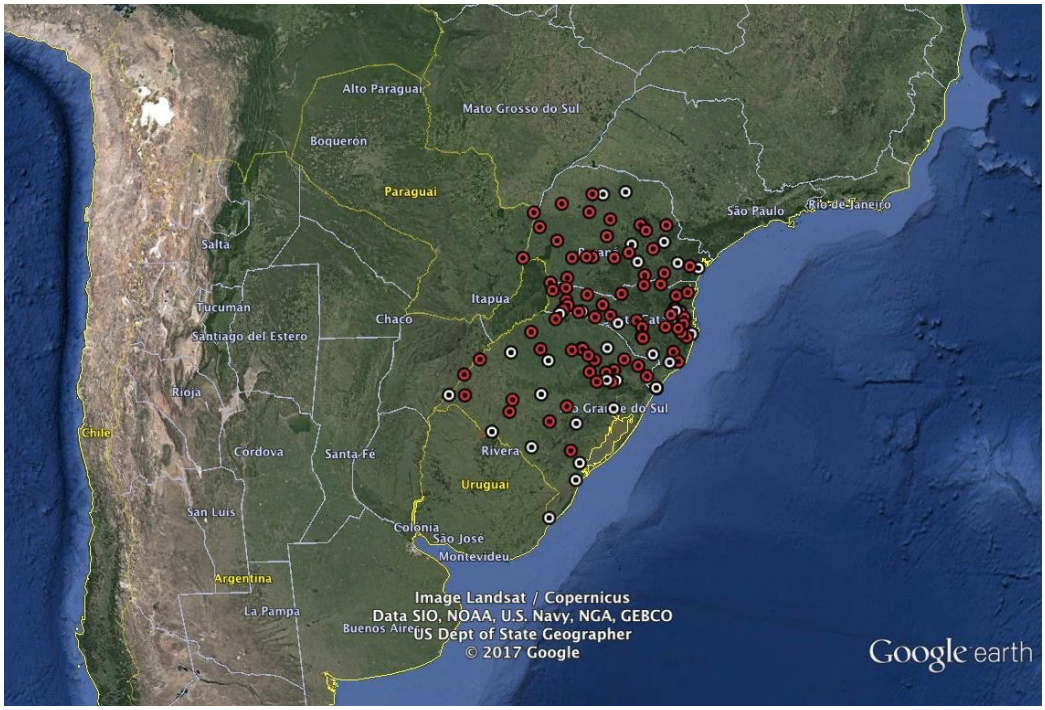

Figure 1: Spatial distribution of rain gauges used in this study. **Note:** (◉): Gauges from the Brazilian meteorological service; (◉): Rain gauges from other sources.

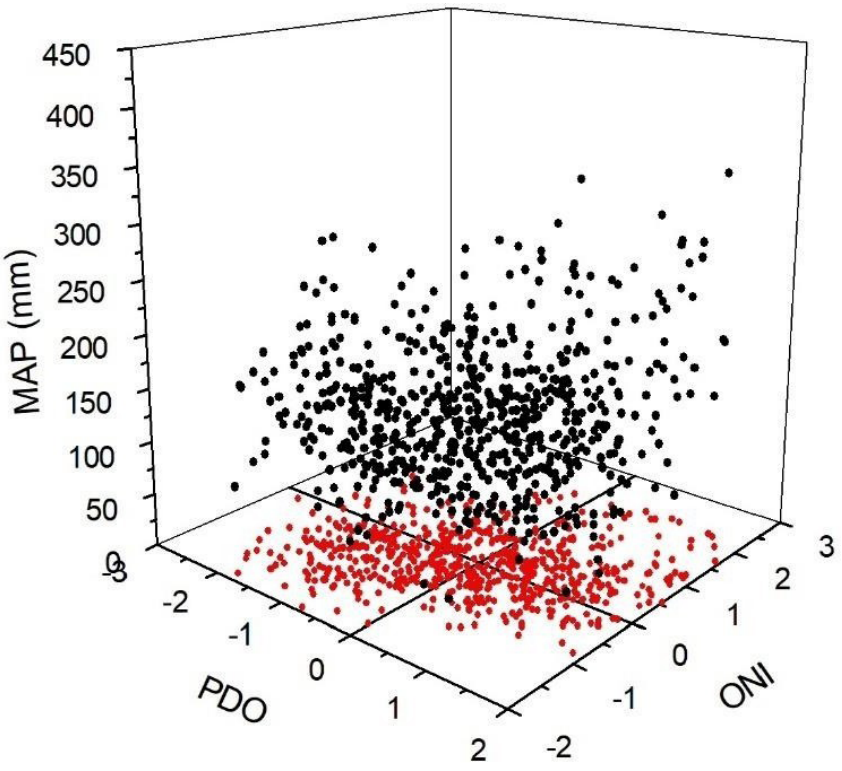

Figure 2: 3D representation of the variables analysed in this article. Monthly average precipitation (black dots) is on the vertical axis, while the corresponding PDO and ONI indices are on the horizontal axes. The red dots are the projection of the black dots on the horizontal plane.

RESULTS AND DISCUSSION

In the following subsections, the analysis is divided into two parts: (a) ENSO and PDO events occurring in one phase, regardless of their intensity and (b) ENSO and PDO events with the highest indices, regardless of their phases. The MAP for the entire region, calculated from the 106 stations between 1961 and 2016, was 140 mm mo^{-1}, taking into account the months with a positive ONI/PDO index, 147/144 mm mo^{-1}, while the months with negative ONI /PDO index had an average of 133/132 mm mo^{-1}. However, it should be emphasized that these values include contributions from all months, including those with neutral conditions. Excluding the neutral months, the MAP for the positive ONI/PDO index was 164/148 mm mo^{-1}, while the value for the negative ONI/PDO index was 136/134 mm mo^{-1}. As can be seen in Figure 3, there was a significant change only in the positive phase of ENSO, despite the exclusion of the neutral months.

Simultaneous impacts of ENSO and PDO events

In this subsection, we consider the combined effects of ENSO and PDO events on Monthly Average Precipitation (MAP), regardless of their intensity. Figure 4 shows the time evolution of MAP and the product between the monthly indices of PDO and ONI, where a positive value indicates that ENSO and PDO are in phase. In this figure, the black dots represent MAP, and the red line denotes the product of the monthly indices of ONI and PDO. From 1961 to 2016, there were many intervals when both indices had the same signal. However, in many of these intervals, the persistence of the phase was observed for a small number of months. This behavior generally occurs when the SST is in a near neutral state and the values of ONI and PDO fluctuate around 0.0. Therefore, only cycles where the phase lasts longer than six months are considered in this section. Within this criterion, there are 21 cycles where the two indices are in phase: 11 with positive values and ten with negative values. These cycles are listed in Table 1. In the columns of the table you will find the number of months in which the phase lasted longer than six months, the MAP for this cycle, the beginning and the decay of the cycle, the range of the indices ONI and PDO, the maximum value of the products ONI and PDO, and the month in which this maximum value occurred. Note that the ranges of PDO and ONI are incomplete for two cycles. This is because one note that the ranges of PDO and ONI are incomplete for

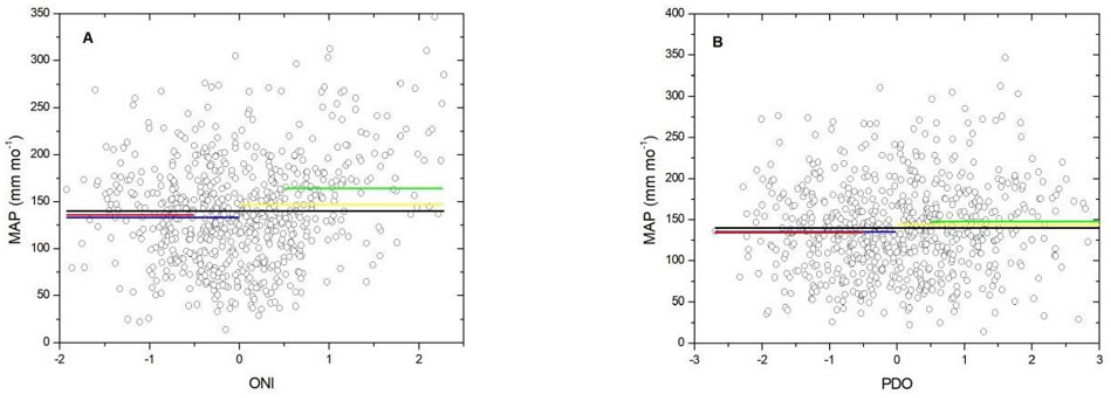

Figure 3: Open circles are MAP values obtained from 106 stations from January 1961 to December 2016. Black line is average precipitation for all periods and all stations of 140 mm mo^{-1}. (a) Yellow and blue lines are averages for months with positive and negative ONI values, respectively. The green and red lines are the averages for the months with ONI>0.5 and <-0.5 values, respectively. (b) The same colors are used to show the averages considering the same limits for PDO.

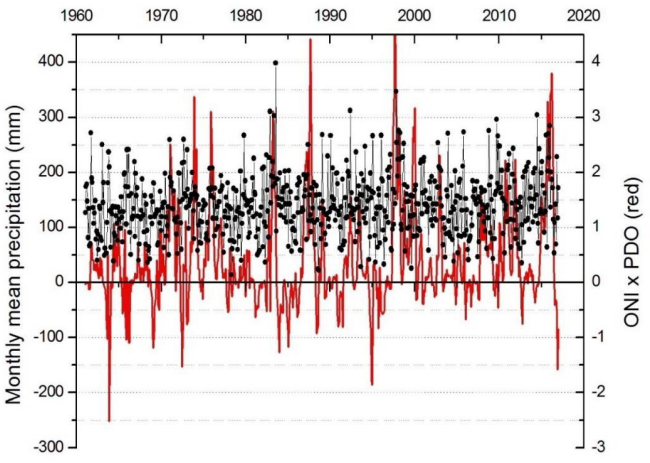

Figure 4: The dots are the Monthly Average Precipitation values (MAP). The red lines represent ONI indices multiplied by PDO indices. Positive values indicate events that are in phase. Negative values indicate cycles of events that are out of phase.

Table 1: Cycles in which ENSO and PDO were in phase for more than 6 months. The first shows the order of the cycles and the months of sustained phase. The second column contains the MAP for that cycle. The third and fourth columns show the onset and decay of the cycle. The fifth and sixth columns show the interval of the ONI and PDO indices in the cycle. The last column contains the maximum value of ONI times PDO and the month in which the maximum was observed.

Cycle/ Month	MAP (mm)	Onset	Decay	Range ONI	Range PDO	Max/Date
01–19	127	Aug-61	Feb-63	(-0.42; -0.11)	(-2.69; -0.16)	0.7 (10/61)
02–11	106	Apr-64	Feb-65	(-0.81; -0.26)	(-1.91; -0.32)	1.14 (12/64)
03–21	123	Sep-66	May-68	(-0.82; 0.0)	(-1.24; -0.05)	0.66 (01/68)
04 – 20	136	Jul-70	Feb-72	(-1.32; -0.36)	(-2.2; xxx)	2.5 (01/71)
05–15	136	May-73	Jul-74	(-1.92; -0.4)	(-1.81; -0.08)	3.3 (11/73)
06–19	138	Dec-74	Jun-76	(-1.57; -0.1)	(-2.08; -0.12)	3.10 (11/75)
07 – 14	135	Jul-76	Aug-77	(0.09; 0.81) W	(0.19; 1.65) S	0.81 (11/76)
08–09	140	Mar-79	Nov-79	(0.10; 0.51) N	(0.17; 1.09) M	0.49 (10/79)
09–13	209	Jul-82	Jul-83	(0.29; 2.12) VS	(xxx; 3.51) VS	3.1 (03/83)
10–21	140	Jul-86	388	(0.12; 1.57) S	(0.22; 2.83) VS	4.41 (08/87)
11–13	155	Aug-91	Aug-92	(0.19; 1.58) S	(0.05; 1.90) S	1.55 (05/92)
12–19	150	Jan-93	Jul-94	(0.11; 0.75) W	(0.05; 2.69) VS	1.59 (05/93)
13–14	188	Apr-97	May-98	(0.14; 2.26) VS	(0.67; 2.79) VS	4.79 (08/97)
14–20	140	Jul-98	02/00	(-1.58; -0.67)	(-2.23; -0.04)	3.16 (01/00)
15–09	137	04-Jan	12-Jan	(-0.36; -0.08)	(-1.37; -0.30)	0.45 (11/01)
16–09	177	08-Feb	04-Mar	(0.02; 1.19) M	(0.42; 2.10) VS	2.31 (12/02)
17–15	120	07-Mar	09-Apr	(0.08; 0.68) W	(0.01; 0.96) W	0.53 (08/04)
18–07	129	01-May	07-May	(0.02; 0.66) W	(0.44; 1.86) S	0.63 (05/05)
19–20	135	09-Jul	04-Sep	(-1.35; -0.08)	(-1.76; -0.36)	1.63(10/07)
20–25	137	06-Oct	06-Dec	(-1.45; -0.12)	(-2.33; -0.22)	2.23 (11/11)
21–22	172	Sep-14	Jun-16	(0.09; 2.28) VS	(0.86; 2.62) VS	3.79 (03/16)

between 1961 and 2016, the ENSO and PDO indices had the same signal for 326 months, with 156 months in the positive phase systematized in 11 cycles and 179 months in the with 156 months in the positive phase systematized in 11 cycles and 179 months in the and the Pacific SST anomalies, the average precipitation was divided into five intervals as shown in Equation 1: ; ; ; ; and ..... (1)

Where is the average in the region of 140 mm mo^{-1}, WB (Well Below) is a MAP value below 98 mm, B (Below) is precipitation between 99 mm and 119 mm, AV (Average) is between 120 and 160 mm, A (Above) is between 161 and 182 mm and WA (Well Above) is precipitation greater than 183 mm.

The intensity of the ENSO and PDO events also had to be classified. For ENSO, the Oceanic Niño index was used, but for PDO events there is no classification system in the literature based on their indices. Therefore, we used the threshold values for ENSO events to classify PDO events as neutral, weak, moderate, strong, or very strong. Positive PDO values are referred to as PDO^+ and negative values as PDO^-. Equation 2 confirms the nine groups used to classify ENSO and PDO intensities:

- i<-2.0 - Very Strong La Niña or PDO^-
- -2.0<i<-1.5 - Strong La Niña or PDO^-
- -1.5<i<-1.0 - Moderate La Niña or PDO^-
- -1.0<i<-0.5 - Weak La Niña or PDO^-
- -0.5<i<0.5 - Neutral
- 0.5<i<1.0 - Weak Niño or PDO^+
- 1.0<i<-1.5 - Moderate Niño or PDO^+
- 1.5<i<2.0 - Strong Niño or PDO^+
- 2.0<i - Very Strong Niño or PDO^+ .....(2)

Using equations 1 and 2, we note that during nine of the ten cycles of negative Pacific SST anomalies, the values of MAP were considered normal (AV) and in six of these cycles there was a solid or moderate Niña concurrent with strong and very strong PDO events. In other words, during the negative Niña and PDO events that were in phase, the monthly average precipitation in southern Brazil from 1961 to 2016 was about average. Therefore, it was not possible to determine whether Niña or PDO^- dominated the mean precipitation in the region. The lowest mean precipitation (106 mm) was observed during a weak La Niña phase with strong PDO^-.

Considering the 11 cycles in which ENSO and PDO occurred together in the positive phase of Pacific SST, in seven of these cycles the mean precipitation values were within the interval considered normal (AV). Three times a strong El Niño and extreme PDO^+ events were observed, in which the mean precipitation values were all above or well above average. However, only these three cycles showed the highest intensities for Niño (ONI>2.0). On the other hand, PDO^+ had its most intense activity (PDO>2.0) during seven cycles, four of which occurred in combination with other ENSO activity (ONI<2.0), in which mean precipitation was within the range of the average. During the 11 cycles in which ENSO and PDO were simultaneously in a positive phase, 36 months had simultaneous indices greater than 1.0. As a result, the average rainfall during these 36 months was 190 mm. Selecting only the 14 simultaneous months with indices corresponding to strong/very strong events (ONI>1.5 and PDO>1.5), the average precipitation was 207 mm.

Periods with extreme values

Because the results of the previous section were inconclusive regarding the modulation effects of PDO on ENSO precipitation, we narrowed the analysis to consider only the extreme indices of ONI and PDO, regardless of whether they were in phase. It was also necessary to define the term "period" for this analysis. Therefore, we defined a "period" as a time interval in which the ENSO or PDO index was higher than a threshold and contained at least one value that exceeded the threshold of 1.5 (-1.5). For this section, the threshold was chosen as one (1.0) for El Niño and PDO$^+$ events and minus one (-1.0) for La Niña and PDO$^-$ events.

Tables 2 and 3 show the months of onset, peak and decay, as well as the length of the period and the maximum index during each period. The column on the right shows the number of months in which the events occurred together. The ONI and PDO indices show three very strong El Niño, four strong La Niña, seven very strong and five strong PDO$^+$, and seven very strong and three strong PDO$^-$ periods. The PDO has a pattern that varies over time; therefore, many of the above periods are part of the same PDO cycle. The main objective of this study was to quantify the individual effects of ENSO and PDO, as well as their combined effects on precipitation. Therefore, we selected months when the index was above or below the threshold. Note that all seven periods where the ONI and PDO are in phase in Table 1 are also included in Tables 2 and 3.

Table 4 shows the MAP values obtained for the periods listed in Tables 2 and 3. In months corresponding to strong and very strong El Niño periods, the MAP estimated by the 106 stations was 186 mm mo^{-1} (32% above average). In periods of very strong Niño, we were at 203 mm mo^{-1} (45% above). The MAP in periods of very strong and strong PDO$^+$ were 157 mm mo^{-1} (12% above) and 161 mm mo^{-1} (15% above), respectively, considering only very strong periods. In months with strong La Niña, the average was 141 mm mo^{-1}. In periods with very strong and strong PDO^{-1}, the MAP was 131 mm mo^{-1}, while periods with strong PDO^{-1} 337 had a MAP of 130 mm mo^{-1}.

The 627 MAPs were analyzed after being classified into two clusters: (a) MAP values that fell within defined ONI or PDO index boundaries and (b) time series of MAPs of approximately

Table 2: Periods, as defined in the text, for which Niño and PDO$^+$ have extreme values. The first/seventh column contains a label for that cycle. Second/eighth column indicates the beginning of the El Niño/PDO$^+$ cycle. Fourth/tenth column the decay of the cycle. Third/ninth column shows the month with the highest value in that cycle. P represents the length of the cycle in months. The last column shows the months in which El Niño and PDO$^+$ were in phase.

El Niño						PDO$^+$						
Cycle	Onset	Peak	Decay	P	Index	Cycle	Onset	Peak	Decay	P	Index	MP
1	Jul-65	Nov-65	Feb-66	8	1.76	-	-	-	-	-	-	0
2	Jul-72	Nov-72	Feb-73	8	1.95	-	-	-	-	-	-	0
-	-	-	-	-	-	3	Oct-76	Jan-77	Feb-77	5	1.65	0
-	-	-	-	-	-	4	Feb-81	May-81	Jun-81	5	1.75	0
5	Aug-82	Dec-82	May-83	10	2.12	6	Feb-83	Jul-83	May-84	16	3.51	3
7	Nov-86	Sep-87	Dec-87	14	1.57	8	Jan-86	Aug-87	May-88	29	2.83	14
9	Nov-91	Jan-92	May-92	7	1.58	-	-	-	-	-	-	0
-	-	-	-	-	-	10	May-92	Jul-92	Aug-92	4	1.9	0
-	-	-	-	-	-	11	Apr-93	Aug-93	May-94	14	2.69	0
-	-	-	-	-	-	12	Apr-95	Jul-95	Jul-95	4	1.71	0
-	-	-	-	-	-	13	Mar-96	May-96	Jun-96	4	2.18	0
14	Jun-97	Nov-97	Mar-98	10	2.26	15	Apr-97	Aug-97	Apr-98	13	2.79	10
-	-	-	-	-	-	16	11-Feb	01-Mar	04-Mar	6	2.1	0
-	-	-	-		-	17	03-May	05-May	06-May	4	1.86	0

Table 3: As in Table 2 for La Niña and PDO$^-$.

LA Niña						PDO$^-$						
Cycle	Onset	Peak	Decay	P	Index	Cycle	Onset	Peak	Decay	P	Index	MP
-	-	-	-	-	-	1	Jul-61	Dec-61	Oct-62	16	-2.69	0
-	-	-	-	-	-	2	Aug-70	Jul-71	Jul-71	12	-2.2	0
-	-	-	-	-	-	3	Oct-71	Mar-72	Jun-72	8	-2.09	0
4	Aug-73	Dec-73	Mar-74	8	-1.92	5	Nov-73	Nov-73	Mar-74	5	-1.81	5
6	Jul-75	Dec-75	Feb-76	8	-1.57	7	Apr-75	Nov-75	Jan-01	12	-2.08	8
8	Jun-88	Dec-88	Mar-89	10	-1.75	-	-	-	-	-	-	0
-	-	-				9	Nov-90	Nov-90	Jun-91	8	-2.23	0
-	-	-				10	Sep-94	Nov-94	Dec-94	4	-1.96	0
11	Jul-99	01/00	03/00	20	-1.58	12	Aug-99	Oct-99	02/00	6	-2.23	6
-	-	-	-	-	-	13	Jul-23	Aug-23	Sep-23	14	-1.76	0
-	-	-	-	-	-	14	Nov-23	Nov-23	Dec-23	15	-2.33	0

Table 4: MAP during the cycles showed in Tables 2 and 3. S and VS means strong or Very Strong events according indexes limits presented in Equation (2).

Positive phase				Negative phase		
El Niño			PDO^+	LA Niña		PDO^-
S and VS (mm m^{-1})	VS (mm m^{-1})	S and VS (mm m^{-1})	VS (mm m^{-1})	S (mm m^{-1})	S and VS (mm m^{-1})	VS (mm m^{-1})
186	Jul-00	Jun-00	Jun-00	141	131	130

equal length. The first approach may be theoretically appropriate, but may have limited accuracy from a mathematical perspective. For example, if equation 2 is used as a framework for classifying ENSO/PDO intensity, the 627 MAP values would be divided into nine/ten groups. Therefore, the number of MAP values with neutral and weak conditions would be much larger than those in strong and very strong limits.

For example, the sample of -05<ONI<0.0 has 183 MAP values, while -1.92<ONI<1.51 has 10 MAP values. The second approach was taken to circumvent this statistical limitation. This involved dividing the same 672 data into ten groups, each of which had approximately the same number of MAP values. The averages estimated in this case may be physically inadequate, but they are statistically more robust. An average value for each block was then calculated for both approaches, and the results are shown in Figure 5. The bars and lines indicate the average values and standard deviations of each block, respectively. The length of each time series is also indicated.

The left panels in Figure 5 show the average precipitation for blocks organized by criteria (a), while the right panels show blocks organized by criteria (b). The top and bottom panels are ONI and PDO, respectively. Figure 5a shows that the average precipitation in the blocks increased significantly from moderate (177 mm mo^{-1}) to strong (184 mm mo^{-1}) and very strong El Niño events (231 mm mo^{-1}) compared to other conditions. However, Figure 5b shows that average precipitation was significantly higher only in the last decade (186 mm mo^{-1}), which is a value of 1.05<ONI<2.28. Since this decade includes moderate, strong, and very strong events, the results shown in Figure 5a are confirmed even when shorter series are used. Figure 5c shows no defined behavior for the average block precipitation when the PDO index is used. The maximum mean precipitation (177 mm mo^{-1}) was in the average range, while in the highest interval the monthly mean precipitation was only 153 mm mo^{-1}. In Figure 5d, the data set was divided into ten blocks of approximately equal length. In the last block, the average (165 mm mo^{-1}) was slightly higher than the averages of the other blocks. The last block in Figure 5d (1.47<PDO<3.51) includes the last two blocks in Figure 5c. For this area of the PDO, the average precipitation across the region was 18% higher than the monthly average precipitation estimated for all data sets (140 mm mo^{-1}). This analysis showed that mean precipitation did not increase appreciably with an increase in the PDO index, as was observed when the ONI index was used. In addition, the standard deviation or variability of precipitation was about the same in the four panels.

Figure 6 shows that monthly average precipitation had a significant positive anomaly only during strong and very strong El Niño events. All MAP values (672) were ordered from lowest to highest regardless of the month of occurrence. That is, the ordering of the data was not a time series. They are shown as circles and are repeated in all panels. The abscissa is the rank of the precipitation amount represented by circles. For example, the lowest MAP was 14 mm (April 1978) and the highest was 398 mm (July 1983). The black line in all panels indicates the average (140 mm mo^{-1}). Figure 6 shows the precipitation amounts in the months of the periods described in Tables 2 and 3. The months corresponding to the cycles of strong and very strong La Niño and PDO^+ are represented by red bars in Figures 6a and 6c, while strong and very strong La Niña and PDO^- months are represented by blue bars in Figures 6b and 6d. Only in the upper left panel (strong and very strong El Niño) was the number of columns that exceeded 140 mm mo^{-1} significantly higher than the number of columns that were below average. In all other fields, this difference was not visually apparent. In the 67 months corresponding to strong and very strong El Niño cycles, precipitation was higher than average (73%) in the other 50 months. Figures 6b, 6c, and 6d show the corresponding percentages of precipitation above and below average. These were 59% to 41%, 61% to 39%, and 58% to 42%, respectively.

Finally, the correlation between the ONI and PDO indices with MAP for the strong and very strong months of the periods is shown in Table 2. The results presented in Figure 7 show a clear upward trend in precipitation when El Niño conditions strengthen, which was not observed during the very strong and strong PDO^+ conditions.

Spatial characteristics

BIn the previous sections, the correlation of the ONI and PDO indices with MAP across the region was analyzed, and the results broadly indicated that only during strong and very strong El Niño months was there a pronounced positive correlation. However, it is not possible to determine whether this general result is the same across all regions or whether parts of the region show correlations under different conditions. These issues are addressed in this section. Figure 8 shows the Monthly Mean Precipitation (MMP) for all stations identified in Figure 1. The green line represents the MMP at each station. The station with the lowest mean (102 mm mo^{-1}) was located at Santa Vitoria do Palmar, the southernmost station (33.52° S), while the highest mean (184 mm mo^{-1}) occurred at Barracão (26.24° S). In the left panel, the red line is the mean value considering only months with strong or very strong Niño, and the blue line is the mean value for months with strong and very strong PDO^+. The MMP was higher than average during extreme El Niño months at all stations and during extreme PDO^+ months. However, this positive anomaly is stronger at the red line than at the blue line. The right panel is similar to the left panel, except for the strong Niña (red line) and very strong and strong PDO^- (blue line). During the strong La Niña and PDO^- months, some stations experienced precipitation deficits and other stations experienced above- average surpluses. The red line is below the green line at 35 stations and the blue line is below the green line at 89 stations. In general, the negative anomaly of precipitation was higher in the PDO extreme months than in the strong Niña months. Only at 12 stations was precipitation lower in La Niña months than in PDO months.

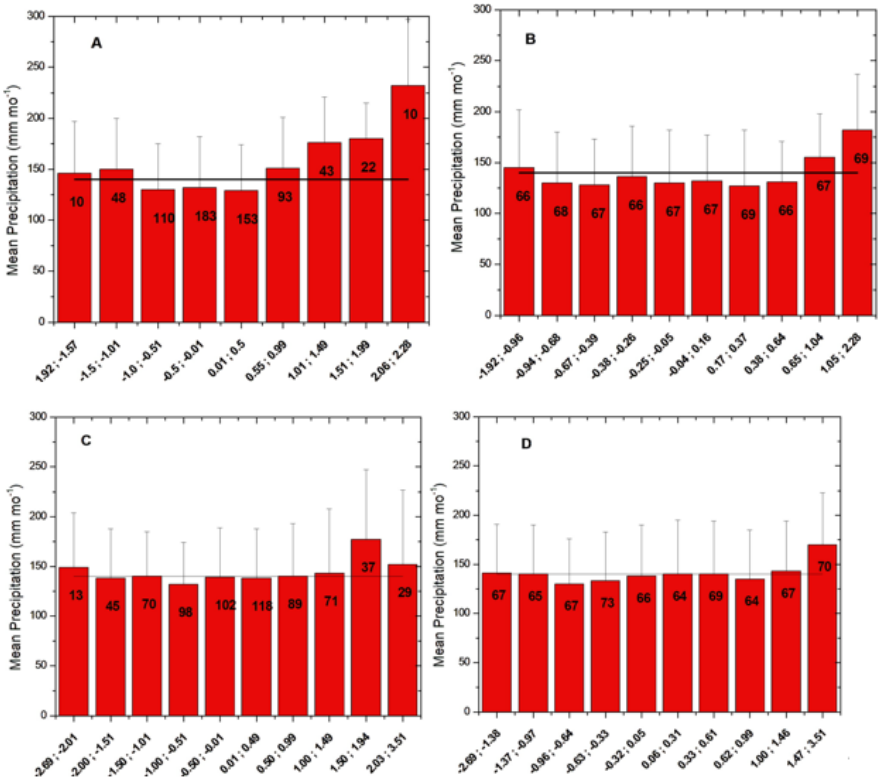

Figure 5: Mean of MAP for two clustering criteria. In figures (a) and (c), the value is obtained when the data are clustered according to the limits of expression 2. In figures (b) and (d), the sample size is approximately the same. On the horizontal axes, the limits of each cluster. The bars represent the standard deviation, while the numbers in the bars indicate the sample size.

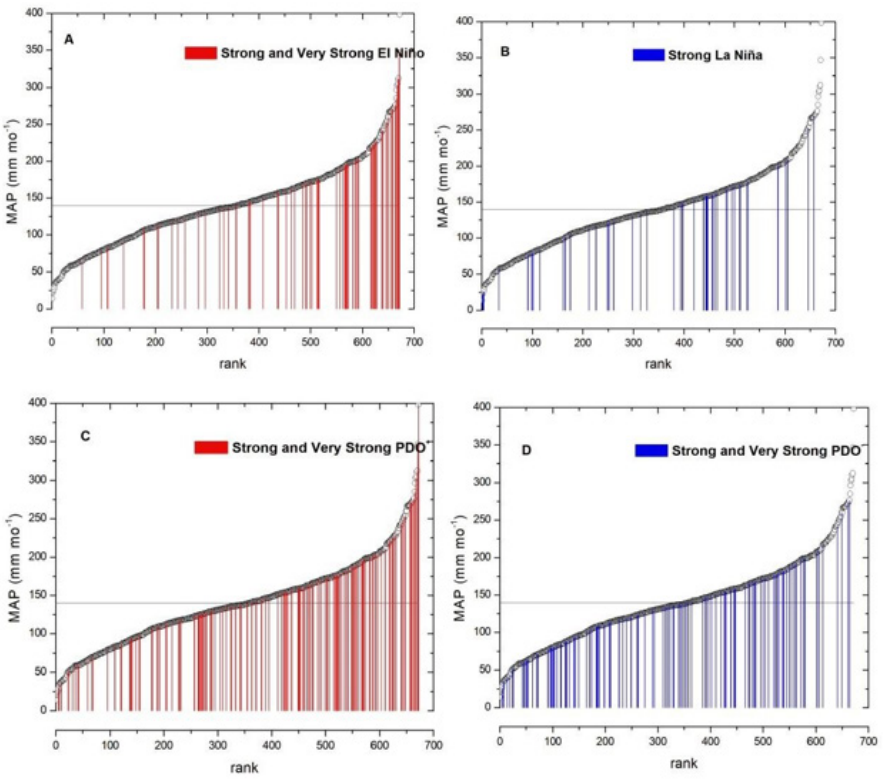

Figure 6: In all figures, the open circles represent the 672 MAP ordered from the lowest (14 mm mo^{-1}) to the highest (398 mm mo^{-1}) value, while the horizontal line represents the average of these 672 values (140 mm mo^{-1}). In figure (a), the vertical red line indicates the months with strong and very strong Niño, while in figure (b) the blue line corresponds to the months with strong Niña. In figures (c) and (d), the red and blue vertical lines correspond to the months with strong and very strong PDO^{+} and PDO^{-}, respectively. **Note:** ( ): Strong and very strong EI Niño; ( ): Strong EI Niña; ( ): Strong and very strong PDO^{+}; ( ): Strong and very strong PDO^{-}.

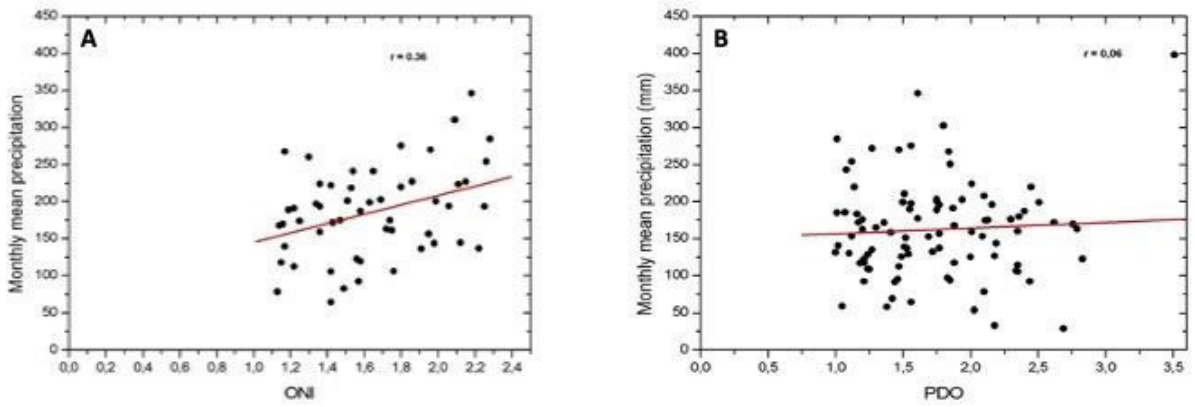

Figure 7: MAP for strong and very strong Niño (a) and strong and very strong PDO$^+$ (b) Red lines are the linear trend. **Note:** (—): Linear trend.

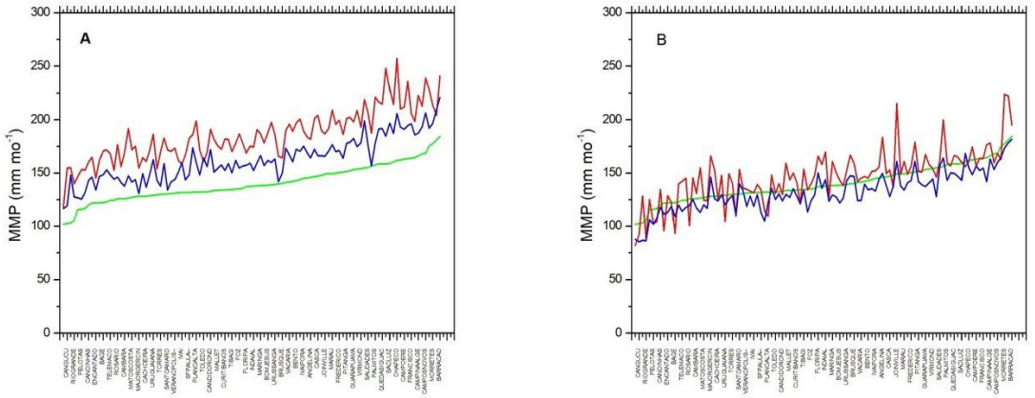

Figure 8: Average of MMP (green line) ordered from lowest to highest. The red and blue lines (a) are the average values of MMP during the months of strong and very strong Niño and strong and very strong PDO$^+$, respectively. The same colors (b) show the average of the MMP during the months with strong Niña and strong and very strong PDO$^-$.

Average monthly anomalies of precipitation in the region are shown in Figure 9. These patterns are not intended to be predictive of expected conditions. However, they use data from 106 precipitation gauges to highlight locations where ENSO and PDO can potentially affect monthly precipitation amounts. From these figures, we can see how SST anomalies in the Pacific affect precipitation in southern Brazil. Strong and very strong El Niño months as shown in Figure 9a increase precipitation across the region, as do events where the monthly PDO$^+$ index exceeds 1.5; however, the impacts vary. The impact of PDO$^+$ as shown in Figure 9b was less than that of Niño. Niño dominated PDO$^+$ even when the two SST anomalies were in phase. The spatial distribution of the PDO$^+$ anomaly was less homogeneous than that of the El Niño months. In other words, the positive precipitation anomaly was not only larger but also more homogeneously distributed across the region in months with very strong and strong El Niño than in months with very strong and strong PDO$^+$. During strong and very strong PDO$^+$ periods, the anomaly was close to zero in coastal areas. Therefore, these events do not appear to affect the average precipitation in this region [46-48].

The effects of a strong La Niña show a well-defined behavior like that of El Niño, but with different characteristics. The anomaly was negative at 35 stations and positive at 71 stations during the months of a strong La Niña, but at 55 of these stations this anomaly ranged from -10 to +10 mm mo^{-1}. The large yellow area indicates the region where this slight anomaly in precipitation occurred in Figure 9b. The relationship between the decrease in precipitation and the intense La Niña periods was evident only in the southern part of the region. In the northern part, the anomaly was positive, in contrast to the data from the south. In other words, the analyzed data set showed a gradient in the precipitation anomaly that decreased from the south to the north of the region. The effects of strong and very strong PDO periods as shown in Figures 9c and 9d, unlike the periods of strong La Niña, did not show a well-defined behavior in precipitation amount, both in terms of intensity and spatial distribution. Like La Niña, the anomaly was negative in the southern part of the region, but responded differently in the northern part.

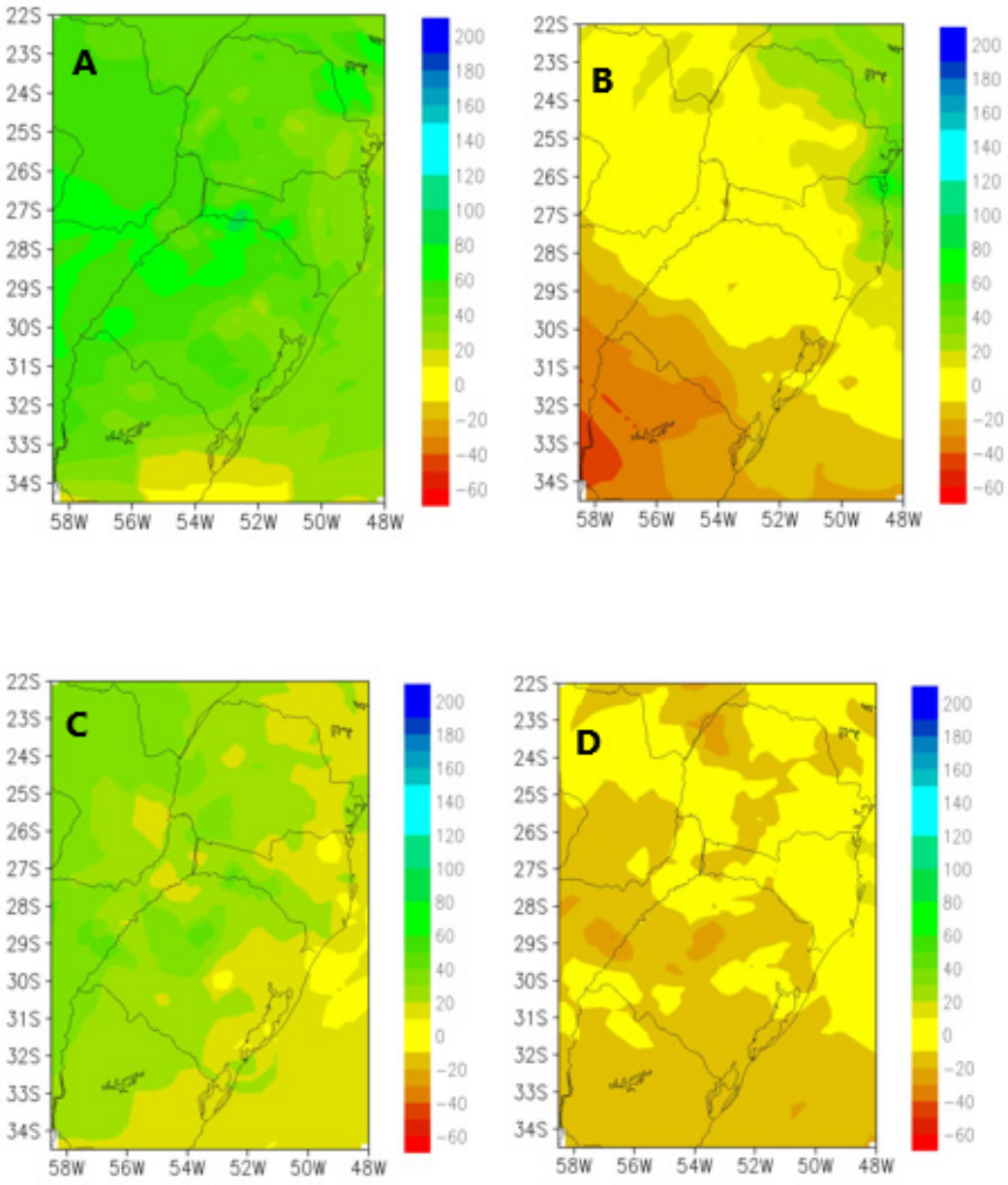

Figure 9: Pattern of monthly precipitation anomaly in the region determined from the 106 monitoring stations for the period 1961-2016 in (a) strong and very strong Niño periods; (b) strong Niña; (c) strong and very strong PDO$^+$; and (d) strong and very strong PDO$^-$. The colour scale is shown in the vertical bars.

CONCLUSION

This study examined precipitation anomalies in southern Brazil using daily precipitation data from 106 monitoring stations from 1961 to 2016. Questions raised relate to the effects of ENSO on precipitation and whether PDO had modulating effects during ENSO events. Monthly average precipitation for each station and the entire region was calculated and correlated with monthly ONI and PDO indices Our results did not show a general pattern of association between El Niño/PDO$^+$ or La Niña/PDO$^-$. Although this study is only a statistical study, it suggests that the combined ENSO-PDO influence on precipitation in the region is weak. This result is due to the fact that the signals associated with these two phenomena are linearly independent. Similar results were reported by Pavia et al, who analyzed the role of PDO and ENSO on the seasonal precipitation anomalies in Mexico. However, a significant correlation was found between anomalous precipitation and climate indices during periods of strong and very strong El Niño events. This behavior was observed throughout the southern region of Brazil. A positive correlation was also present for periods of strong and very strong PDO$^+$, but it was less significant than the previous correlation. The results showed that El Niño events were predominant during the much longer positive phase of PDO. The opposite was observed for La Niña events, which were not dominant during the longer negative phase of PDO events. The decrease in precipitation was more homogeneous during strong and very strong PDO events than during strong La Niña events. The correlation between negative precipitation anomalies during strong La Niña periods can be described as a gradient from positive in the south to negative

in the north of the southern region. In the central part of the southern region, this correlation was absent or very low. The precipitation anomaly was more significant the higher the index ONI was, and was about 45% higher in the months with very strong El Niño than the MAP determined for the entire period. This positive anomaly was observed at all 106 meteorological stations. These data may be sufficient for agricultural, water use, drainage and emergency management stakeholders to consider the possibility of high precipitation events during these months. However, it is difficult to determine if the increased precipitation will be in the form of heavy precipitation events concentrated over a few days. Positive precipitation anomalies were also observed at all meteorological stations during the heavy and very heavy PDO^+ months, but their maximum was only 15% higher than that of MAP. The increase in precipitation during strong and very strong El Niño events was more pronounced than the increase in precipitation during strong and very strong PDO^+ events. As indicated earlier, the anomaly in precipitation during months of strong La Niña or strong PDO is negative at some meteorological stations and positive at others. Finally, it is important to emphasize that the results of this study stand out from others because they are based on long time series from a wide observational network. Similar available studies rely on sparse observations or numerical models. Our data-driven approach allows us to provide insights and results that are not only accurate, but also highly reliable.

ACKNOWLEDGMENTS

This work was supported by the National Institute of Science and Technology for Climate Change phase 2 under CNPq Grant 465501/2014-1, FAPESP Grants 2014/50848-9, 2015/50122-0, 2015/03804-9 and 2017/09659-6; the National Coordination for High Level Education and Training (CAPES) Grant.

REFERENCES

1. Brasil IB. Instituto Brasileiro de geografia e Estatística. Censo Demográ. 2010;2010:11.
2. Liebmann B, Mechoso CR. The South American monsoon system. Global Monsoon Sys: Res Forec. 2011:137-157.
3. Kousky VE, Kagano MT, Cavalcanti IF. A review of the Southern Oscillation: Oceanic-atmospheric circulation changes and related rainfall anomalies. Tellus A. 1984;36(5):490-504.
4. Rao VB, Hada K. Characteristics of rainfall over Brazil: Annual variations and connections with the Southern Oscillation. Theor Appl Climatol. 1990;42:81-91.
5. Mechoso CR, Iribarren GP. Streamflow in Southeastern South America and the Southern oscillation. J Clim. 1992:1535-1539.
6. Grimm AM, Ferraz SE, Gomes J. Precipitation anomalies in Southern Brazil associated with El Niño and La Niña events. J Clim. 1998;11(11):2863-2880.
7. Grimm AM, Barros VR, Doyle ME. Climate variability in Southern South America associated with El Niño and La Niña events. J Clim. 2000;13(1):35-58.
8. Aceituno P. On the functioning of the Southern Oscillation in the South American sector. Part I: Surface climate. Mon Weather Rev. 1988;116(3):505-524.
9. Diaz AF, Studzinski CD, Mechoso CR. Relationships between precipitation anomalies in Uruguay and Southern Brazil and sea surface temperature in the Pacific and Atlantic Oceans. J Clim. 1998;11(2):251-271.
10. Ambrizzi T, de Souza EB, Pulwarty RS. The Hadley and Walker regional circulations and associated ENSO impacts on South American seasonal rainfall. Hadley Circulat. 2004:203-235.
11. Grimm AM. The El Niño impact on the summer monsoon in Brazil: Regional processes versus remote influences. J Clim. 2003;16(2):263-280.
12. Grimm AM, Ambrizzi T. Teleconnections into South America from the tropics and extratropics on interannual and intraseasonal timescales. Past Clim Variabil Regi. 2009:159-191.
13. Pscheidt I, Grimm AM. Frequency of extreme rainfall events in Southern Brazil modulated by interannual and interdecadal variability. Int J Climatol. 2009;29(13):1988-2011.
14. Grimm AM, Tedeschi RG. ENSO and extreme rainfall events in South America. J Clim. 2009;22(7):1589-1609.
15. Rao VB, Franchito SH, Santo CM, Gan MA. An update on the rainfall characteristics of Brazil: Seasonal variations and trends in 1979–2011. Int J Climatol. 2016;36(1):291-302.
16. Cai W, McPhaden MJ, Grimm AM, Rodrigues RR, Taschetto AS, Garreaud RD, et al. Climate impacts of the El Niño–Southern Oscillation on South America. Nature Rev Earth Environ. 2020;1(4):215-231.
17. Almazroui M, Ashfaq M, Islam MN, Rashid IU, Kamil S, Abid MA, et al. Assessment of CMIP6 performance and projected temperature and precipitation changes over South America. Earth Sys Environ. 2021;5(2):155-183.
18. Vera C, Silvestri G. Precipitation interannual variability in South America from the WCRP-CMIP3 multi-model dataset. Clim Dynam. 2009;32:1003-1014.
19. Saji NH, Ambrizzi T, Ferraz SE. Indian Ocean dipole mode events and austral surface air temperature anomalies. Dyn Atmos Oceans. 2005;39(1-2):87-101.
20. Andreoli RV, Kayano MT. ENSO-related rainfall anomalies in South America and associated circulation features during warm and cold Pacific decadal Oscillation regimes. Int J Climatol. 2005;25(15):2017-2030.
21. Kayano MT, Capistrano VB. How the Atlantic Multidecadal Oscillation (AMO) modifies the ENSO influence on the South American rainfall. Int J Climatol. 2014;34(1):162-178.
22. Fernandes LG, Rodrigues RR. Changes in the patterns of extreme rainfall events in southern Brazil. Int J Climatol. 2018;38(3):1337-1352.
23. Garreaud RD, Boisier JP, Rondanelli R, Montecinos A, Sepúlveda HH, Veloso-Aguila D. The central Chile mega drought (2010–2018): A climate dynamics perspective. Int J Climatol. 2020;40(1):421-439.
24. Power S, Casey T, Folland C, Colman A, Mehta V. Inter-decadal modulation of the impact of ENSO on Australia.

Clim Dynam. 1999;15:319-324.

25. Levine AF, McPhaden MJ, Frierson DM. The impact of the AMO on multidecadal ENSO variability. Geophys Res Lett. 2017;44(8):3877-3886.
26. Reboita MS, Ambrizzi T, Crespo NM, Dutra LM, Ferreira GW, Rehbein A, et al. Impacts of teleconnection patterns on South America climate. Ann N Y Acad Sci. 2021;1504(1):116-153.
27. Schoennagel T, Veblen TT, Romme WH, Sibold JS, Cook ER. ENSO and PDO variability affect drought-induced fire occurrence in Rocky Mountain subalpine forests. Ecol Appl. 2005;15(6):2000-2014.
28. McCabe GJ, Ault TR, Cook BI, Betancourt JL, Schwartz MD. Influences of the El Niño Southern Oscillation and the Pacific Decadal Oscillation on the timing of the North American spring. Int J Climatol. 2012;32(15):2301-2310.
29. Henson C, Market P, Lupo A, Guinan P. ENSO and PDO related climate variability impacts on Midwestern United States crop yields. Int J Biometeorol. 2017;61:857-867.
30. Mariano E, Carolina V, Miranda Leandro A. Influences of ENSO and PDO phenomena on the local climate variability can drive extreme temperature and depth conditions in a Pampean shallow lake affecting fish communities. Environ Biol Fishes. 2018;101:653-666.
31. Nguyen PL, Min SK, Kim YH. Combined impacts of the El Niño-Southern Oscillation and Pacific decadal oscillation on global droughts assessed using the standardized precipitation evapotranspiration index. Int J Climatol. 2021;41:E1645-E1662.
32. Gamelin BL, Carvalho LM, Kayano M. The combined influence of ENSO and PDO on the spring UTLS ozone variability in South America. Climate Dyna. 2020;55:1539-1562.
33. Wang X, Liu H. PDO modulation of ENSO effect on tropical cyclone rapid intensification in the Western North Pacific. Clim Dynam. 2016;46:15-28.
34. Xue X, Chen W, Chen S, Feng J. PDO modulation of the ENSO impact on the summer South Asian high. Clim Dynam. 2018;50:1393-1411.
35. Zeng Y, Huang C, Tang Y, Peng J. Precipitation variations in the flood seasons of 1910–2019 in Hunan and its association with the PDO, AMO, and ENSO. Front Earth Sci. 2021;9:656594.
36. Li S, Xiao Z, Zhao Y. Combined effect of the PDO and ENSO on the date of the first tropical cyclone landfall in continental East Asia. J Geophys Res Atmos. 2021;126(9):e2020JD034059.
37. Huang C, Liu H, Wang X, Li H, Zhang Z, Zuo J, et al. PDO modulation on the relationship between ENSO and typhoon tracks. J Clim. 2022;35(20):6703-6720.
38. Grimm AM, Laureanti NC, Rodakoviski RB, Gama CB. Interdecadal variability and extreme precipitation events in South America during the monsoon season. Clim Res. 2016;68(2-3):277-294.
39. Penalba OC, Rivera JA, Pántano VC, Bettolli ML. Extreme rainfall, hydric conditions and associated atmospheric circulation in the Southern La Plata Basin. Clim Res. 2016;68(2-3):215-229.
40. Tedeschi RG, Cavalcanti IF, Grimm AM. Influences of two types of ENSO on South American precipitation. Int J Climatol. 2013;33(6):1382-1400.
41. Jimenez JC, Marengo JA, Alves LM, Sulca JC, Takahashi K, Ferrett S, et al. The role of ENSO flavours and TNA on recent droughts over Amazon forests and the Northeast Brazil region. Int J Climatol. 2021;41(7):3761-3780.
42. Silva ME, Silva CB, Ambrizzi T, Drumond A, Patucci NN. South America climate during the 1970–2001 Pacific Decadal Oscillation phases based on different reanalysis datasets. Front Earth Sci. 2020;7:359.
43. Villamayor J, Ambrizzi T, Mohino E. Influence of decadal sea surface temperature variability on Northern Brazil rainfall in CMIP5 simulations. Clim Dynam. 2018;51:563-579.
44. Silva VB, Kousky VE, Higgins RW. Daily precipitation statistics for South America: An intercomparison between NCEP reanalyses and observations. J Hydrometeorol. 2011;12(1):101-117.
45. Mantua NJ, Hare SR, Zhang Y, Wallace JM, Francis RC. A Pacific interdecadal climate oscillation with impacts on salmon production. Bull Am Meteorol Soc. 1997;78(6):1069-1080.
46. Glantz MH, Ramirez IJ. Reviewing the Oceanic Niño Index (ONI) to enhance societal readiness for El Niño's impacts. Int J Disaster Risk Sci. 2020;11:394-403.
47. Kalkstein AJ, Goodrich GB. The effect of ENSO and PDO on three airborne pollutants in Phoenix, Arizona. J Ariz-Nev Acad Sci. 2012;43(2):91-98.
48. Pavia EG, Graef F, Reyes J. PDO–ENSO effects in the climate of Mexico. J Clim. 2006;19(24):6433-6438.